Chemical Physics 357 (2009) 17–20

Contents lists available at ScienceDirect

Chemical Physics

journal homepage: www.elsevier.com/locate/chemphys

Exciton migration and fluorescence quenching in LHCII aggregates: Target analysis using a simple nonlinear annihilation scheme

Leonas Valkunas [a,*], Ivo H.M. van Stokkum [b], Rudi Berera [b], Rienk van Grondelle [b]

[a] Institute of Physics, Savanoriu 231, LT-02300 Vilnius, Lithuania and Department of Theoretical Physics, Faculty of Physics, Vilnius University, Sauletekio 9, LT-10222 Vilnius, Lithuania
[b] Department of Physics and Astronomy, Faculty of Sciences, VU University of Amsterdam, De Boelelaan 1081, 1081 HV Amsterdam, The Netherlands

ARTICLE INFO

Article history:
Received 5 June 2008
Accepted 27 July 2008
Available online 19 August 2008

Keywords:
Non-photochemical quenching
Exciton–exciton annihilation
Target analysis
Transient spectra
.

ABSTRACT

When exposed to excess light illumination photosynthetic organisms switch into a photoprotective quenched state where the excess energy is safely dissipated as heat. When these processes are investigated by means of ultrafast spectroscopy, the experimentalist is faced with the unnatural process of singlet–singlet annihilation which often makes the interpretation of the results very complicated.

It was recently discovered that the main light-harvesting complex of plants, LHCII, plays a key role in the dissipation of excess energy in the process of non-photochemical quenching. Here we demonstrate that the excitation kinetics in the quenched state can be described by a simple model, which assumes specific trapping centers to be present in the system. In order to explain the experimental results a physical model for exciton–exciton annihilation is applied. Besides providing a more detailed interpretation of the kinetic data, the model provides a general annihilation scheme which can potentially be applied to a number of systems provided the pool of pigments is sufficiently large.

1. Introduction

In plant photosynthesis a membrane-bound light-harvesting apparatus efficiently collects solar photons and delivers the excitation energy to the reaction centers [1]. Typically about 200–300 chlorophylls and carotenoids cooperate thereby driving the essential photochemical reactions at an acceptable rate even at low light intensities. However at high light intensities the electron transport chain becomes saturated and in particular the formation of triplet states by charge recombination in the photosystem II (PSII) reaction center (RC) poses a serious problem. This is because in the PSII RC triplet transfer to a carotenoid does not occur and consequently singlet oxygen is produced [2]. To deal with this excess excitation energy plants have evolved a physiologically vital strategy which allows them to regulate their light-harvesting capacity [3]. Under high light conditions a dissipative process in the light-harvesting antenna of PSII is switched on, and the excess excitation energy is dissipated as heat, a phenomenon generally known as non-photochemical quenching (NPQ). Due to this capacity to rapidly adapt to large variations in the light environment, plant photosynthesis may function under very different light conditions and this property significantly contributes to their fitness [4]. Recent studies have demonstrated that carotenoids can potentially quench the chlorophyll (Chl) excited state via charge transfer [5] or energy relaxation [6] mechanisms. A key role in this regulatory process is played by the main light-harvesting complexes of PSII, LHCII, which under high light conditions is able to switch into a dissipative mode. It was shown that in quenched LHCII the Chl excited state decays via energy transfer to one of the luteins (lut1) in the complex [7], a process very similar to that earlier observed in carotenoo-phthalocyanine dyads [6].

However, both in quenched thylakoids [5] and in quenched LHCII complexes [7] very complex excited state kinetics were observed, amongst others depending on the spectral region that is probed. For instance, in the analysis of the time-resolved spectra of quenched LHCII a compartmental model was used that included different populations of Chls to account for the observed multi-exponential decay (cf. Fig. S3). A specific feature of quenched thylakoids and LHCII aggregates is that they contain a substantial amount of connected pigments, and therefore under the conditions used for these experiments (about 1 excitation per 100 Chls) nonlinear excitation decay channels caused by singlet–singlet annihilation [8] or singlet–triplet annihilation [9] should be taken into account when describing the excitation relaxation. To correctly quantify the yield of all the possible relaxation channels a physically relevant model should be used. In this paper we demonstrate that it is possible to explain the experimentally observed kinetics obtained in LHCII aggregates under quenched conditions by using a physical model for multi-excitation annihilation that is fully consistent with our previous studies on LHCII aggregates [8].

* Corresponding author.
E-mail address: leonas.valkunas@ff.vu.lt (L. Valkunas).

0301-0104/$ - see front matter © 2008 Elsevier B.V. All rights reserved.
doi:10.1016/j.chemphys.2008.07.025

2. Kinetic model

To describe the excited state decay kinetics in quenched LHCII aggregates on a timescale from picoseconds to hundreds of picoseconds we adopt a model where exciton decay can occur by energy transfer to some specific quenchers responsible for NPQ, by intersystem crossing to a triplet state, fluorescence and internal conversion and by singlet–singlet annihilation. Thus, to describe the exciton evolution in LHCII aggregates on the time scale characteristic for the exciton migration between LHCII monomers the following kinetic equations should be used [8]:

$$\frac{dn}{dt} = -\frac{\gamma}{2}n^2 - (k_Q + k_T)n, \quad (1)$$

$$\frac{dn_Q}{dt} = k_Q n - k_R n_Q, \quad (2)$$

$$\frac{dn_T}{dt} = k_T n - K n_T, \quad (3)$$

where n is the exciton concentration, n_Q is the concentration of the excitons trapped by the quencher, k_Q is the rate at which the excitons are trapped by the quencher, k_R is the relaxation of the trapped excitons, γ defines the rate of exciton–exciton annihilation, n_T determines the triplet concentration, k_T is the rate of the intersystem crossing, internal conversion and fluorescence (below we will assume that a fraction 0.5 actually forms triplets) and K is the rate of triplet decay. The exciton equilibration within an individual LHCII complex which takes place within 1–2 ps will be incorporated below.

The analytical solution of Eq. (1) for a certain number of initial excitations n_0 (determined by the intensity of the excitation pulse) is given by:

$$n(t) = \frac{n_0 e^{-(k_T+k_Q)t}}{1 + \frac{n_0\gamma/2}{k_T+k_Q}(1 - e^{-(k_T+k_Q)t})}, \quad (4)$$

Note that the shape of $n(t)$ depends upon γn_0, which is the product of the value determining the rate of exciton–exciton annihilation and the initial exciton concentration, and upon the sum of the decay rates $k_Q + k_T$.

Subsequent numerical integration, by substituting Eq. (4) into Eqs. (2) and (3), results in the following solutions:

$$n_Q(t) = k_Q e^{-k_R t} \int_0^t n(t') e^{k_R t'} dt', \quad (5)$$

and

$$n_T(t) = k_T e^{-Kt} \int_0^t n(t') e^{Kt'} dt'. \quad (6)$$

Eqs. (1)–(3) have been implemented in a target model similar to the one used previously but with one major difference: the two chlorophyll compartments that were necessary in Ruban et al. [7] to describe the multi-exponential nature of the Chl excited state decay, have been replaced by one compartment that now contains a physical model for annihilation according to Eq. (1). The compartmental model is shown in Fig. 1. The first compartment describes the excited states of LHCII, with ultrafast equilibration within an individual (monomeric) complex (rate constant k_1). The second compartment reflects the spectrally equilibrated state of the LHCII aggregates with excitons hopping around from monomer to monomer until they reach a quenching site, or until they meet a second exciton and one is annihilated or until they decay by internal conversion, fluorescence or triplet formation. In Figs. 1–3 the following colors are used for the four different species: unrelaxed Chl (green), relaxed Chl (red), quencher Q (blue) and triplet state (cyan). All the parameters of the model including the species associated difference spectra (SADS) of the various states are estimated from a global fit

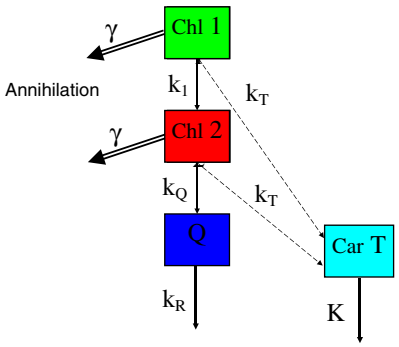

Fig. 1. Compartmental scheme used with target analysis. Left pointing arrows represent annihilation, right pointing arrows represent triplet formation (with quantum yield 0.5), remainder is internal conversion and fluorescence. For clarity we left out a very small path with rate k_Q from Chl1 to Q.

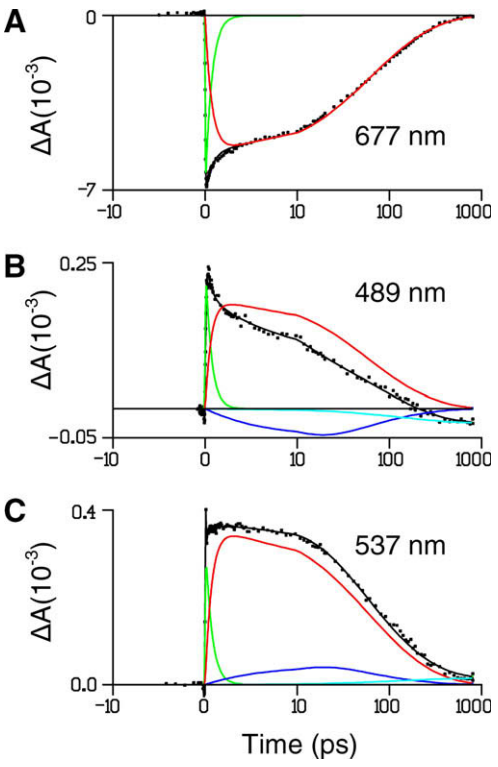

Fig. 2. Target analysis results at 677, 489 and 537 nm. Solid black curve represents fit to data points. The time axis is linear till 10 ps and logarithmic thereafter. Chl1, Chl2, Q and T contributions are indicated by green, red, blue and cyan curves.

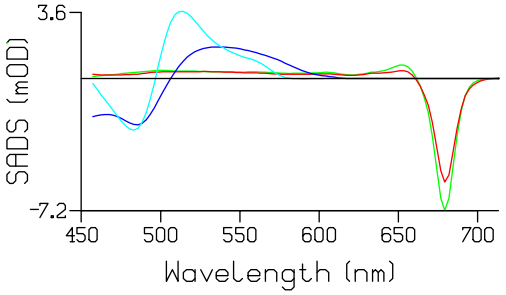

Fig. 3. Target analysis results for sample 1. Estimated Chl1, Chl2, Q and T species associated difference spectra (SADS) are indicated by, respectively, green, red, blue and cyan curves.

of the data [10]. This annihilation model not only represents a more accurate description of the underlying physics but at the same time reduces the number of free parameters in the estimate. Note that with an instrument response function (IRF) of finite width no analytical solution of Eq. (1) is possible, and all differential equations have to be integrated numerically. This requires the use of numerical methods that can deal with this so-called stiff problem.

3. Results and discussion

The target analysis was applied to two different, strongly quenched samples. In Fig. 2A–C the fits of kinetic traces at three informative wavelengths are shown from the first sample, that were also shown previously [7]. The 677 nm trace (Fig. 2A) displays pure chlorophyll Q_y decay and contains no contribution from the quenching state. The trace at 489 nm (Fig. 2B) is taken as representative of the carotenoid ground state bleach superimposed on chlorophyll *a* (Chl*a*) excited state absorption. The trace at 537 nm (Fig. 2C) on the other hand represents carotenoid excited state absorption superimposed on Chl*a* excited state absorption [7]. At late times a carotenoid triplet state also contributes at 489 and 537 nm. The estimated contributions of each species to the fit are indicated by the respective colors.

The kinetic parameters estimated from this global analysis are collated in Table 1. In particular we estimate $(\gamma n_0/2)^{-1} = 69 \pm 10$ ps, $k_Q^{-1} = 270 \pm 70$ ps. Note that the quencher lifetime was fixed, $k_R^{-1} = 8$ ps (this does not affect the quality of the fit). The SADS estimated from the fit are shown in Fig. 3. The spectra are essentially identical to those estimated earlier from the five compartment model depicted in Fig. S3 [7]. In Fig. S1 the same analysis was applied to another strongly quenched sample. The results are completely consistent, the SADS in Fig. S2 are very similar to those in Fig. 3, and the same kinetic parameters were estimated, except for a different k_1 (0.7 vs 1.4/ps). Therefore in Table 1 we report a relatively large error margin of k_1. The shape of the Q SADS (blue in Fig. S2) is slightly different, which is not surprising since this is only a small contribution to the signal.

Previously, the mean time of exciton–exciton annihilation was estimated to be $\gamma^{-1} = 16$ ps when normalizing them per trimer of the LHCII complexes [8]. Here we estimate $(\gamma n_0/2)^{-1} = 69 \pm 10$ ps. Thus for these results to be consistent we must have $n_0 \approx 0.46$, which means that we excite approximately half of the trimers. From our estimate $k_Q^{-1} \approx 270$ ps and we conclude that trapping centers are present in only a small fraction of the trimers. Thus within the framework of our model, the quenching of Chl excited state energy reflects an inverted kinetics process, where the quenching state is slowly populated and quickly depopulated and thereby attains an intrinsically low transient concentration.

3.1. Role of heterogeneity

In Fig. S3 the compartmental model used in [7] is shown. Note that five rate constants ($k_1 - k_5$) are needed to describe the Chl spectral relaxation ($k_1 + k_2 + k_3$), annihilation (k_4 and k_5) and heterogeneity. In particular k_3 determines the excitation relaxation pathway in unquenched conditions, which is the dominant fraction in less quenched samples. So only with a strongly quenched sample the homogeneous annihilation model (which has just three parameters k_1, k_Q and γ for Chl) is adequate. To describe less quenched samples heterogeneity will be needed, and the number of compartments and parameters increases again: one extra parameter is needed to account for an unquenched fraction, and possibly the annihilation rate differs.

Table 1
Parameters estimated from target analysis of two strongly quenched samples

Parameter	Rate in 1/ps
k_1	1.0 ± 0.3
k_Q	0.0038 ± 0.0010
k_T	0.0002 (fixed)
k_R	0.125 (fixed)
K	0.000001 (fixed)
$\gamma n_0/2$	0.014 ± 0.002

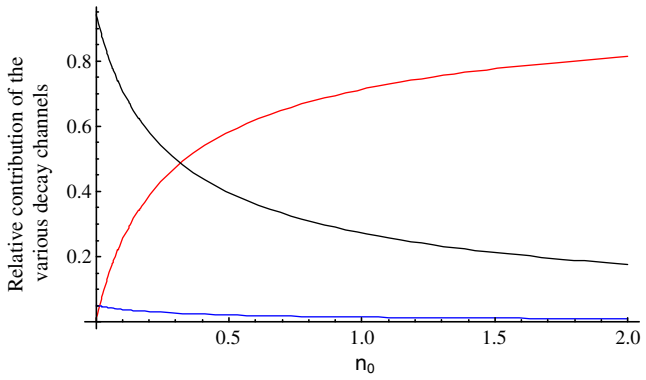

Fig. 4. Relative contribution of the various decay channels: non-photochemical quenching via the quenching state (black), decay via singlet–singlet annihilation (red) and decay via a triplet state (blue). (For interpretation of the references to colour in this figure legend, the reader is referred to the web version of this article.)

3.2. System behaviour with increasing light

Having estimated the system parameters γn_0 and k_Q that describe the dynamics we can now calculate how the contributions of the various decay channels change as a function of the light intensity. In experiments increasing the excitation power increases n_0. Fig. 4 shows the relative contributions of the various decay channels, i.e. non-photochemical quenching via the quenching state (black curve), decay via singlet–singlet annihilation (red) and decay via the triplet formation (blue) as a function of n_0 (assuming that $\gamma^{-1} = 16$ ps [8]). The decay via the quenching state represents the main decay channel for values of n_0 smaller than about 0.3. In natural conditions trapping by open reaction centers is present, and the excitations are continuous in time, thus Eq. (1) should be modified accordingly:

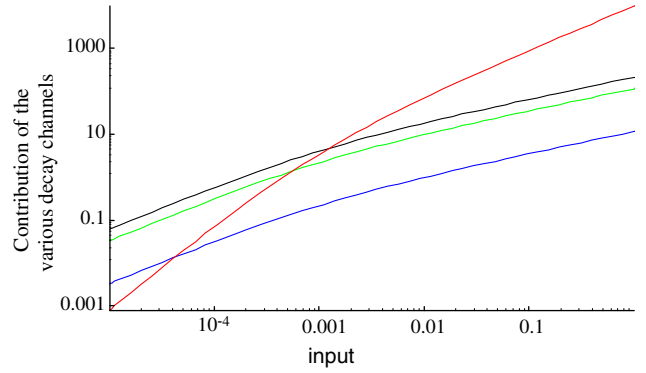

Fig. 5. Contribution of the various decay channels at steady state as a function of input light intensity. Key: non-photochemical quenching via the quenching state (black), decay via singlet–singlet annihilation (red), decay via triplet state formation (blue), photochemical quenching via charge separation (green). (For interpretation of the references to colour in this figure legend, the reader is referred to the web version of this article.)

$$\frac{dn}{dt} = -\frac{\gamma}{2}n^2 - (k_Q + k_T + k_{RC})n + \text{input}, \quad (7)$$

where k_{RC} is the rate of trapping by open reaction centers (assumed to be 1/(500 ps)), and the input is assumed a constant. Fig. 5 depicts the contribution of the various decay channels at steady state as a function of the input light intensity. Note that for low light intensity (below 0.001) the quenching state represents the main decay channel. Natural light intensities are well below 0.0001.

4. Conclusions

We have shown that the multi-exponential decay of the Chl excited state in strongly quenched LHCII aggregates can be fully described by a physical annihilation model, provided that the estimated values for n_0 and k_Q are realistic. It is noteworthy that in this kinetic model the rate of exciton–exciton annihilation γ was taken to be identical to that obtained from earlier independent experimental data [8] and consistent with known migration time of about 5 ps between monomers [8]. Besides providing a more detailed interpretation of the kinetic data, the model provides a general annihilation scheme which can potentially be applied to a number of systems provided the pool of pigments is sufficiently large.

Acknowledgements

This research was supported by The Netherlands Organization for Scientific Research (NWO) via the Dutch Foundation for Earth and Life Sciences (ALW) and by the Lithuanian State Science and Studies Foundation.

Appendix A. Supplementary material

Supplementary data associated with this article can be found, in the online version, at doi:10.1016/j.chemphys.2008.07.025.

References

[1] R. van Grondelle, J.P. Dekker, T. Gillbro, V. Sundström, Biochim. Biophys. Acta 1187 (1994) 1.
[2] J. Barber, B. Andersson, Trends Biochem. Sci. 17 (1992) 61.
[3] P. Horton, A.V. Ruban, R.G. Walters, Annu. Rev. Plant Physiol. Plant Mol. Biol. 47 (1996) 655.
[4] C. Kulheim, J. Agren, S. Jansson, Science 297 (2002) 91.
[5] N.E. Holt, D. Zigmantas, L. Valkunas, X.P. Li, K.K. Niyogi, G.R. Fleming, Science 307 (2005) 433.
[6] R. Berera, C. Herrero, I.H.M. van Stokkum, M. Vengris, G. Kodis, R.E. Palacios, H. van Amerongen, R. van Grondelle, D. Gust, T.A. Moore, A.L. Moore, J.T.M. Kennis, Proc. Natl. Acad. Sci. USA 103 (2006) 5343.
[7] A.V. Ruban, R. Berera, C. Ilioaia, I.H.M. van Stokkum, J.T.M. Kennis, A.A. Pascal, H. van Amerongen, B. Robert, P. Horton, R. van Grondelle, Nature 450 (2007) 575.
[8] V. Barzda, V. Gulbinas, R. Kananavicius, V. Cervinskas, H. van Amerongen, R. van Grondelle, L. Valkunas, Biophys. J. 80 (2001) 2409.
[9] V. Barzda, M. Vengris, L. Valkunas, R. van Grondelle, H. van Amerongen, Biochemistry 39 (2000) 10468.
[10] I.H.M. van Stokkum, D.S. Larsen, R. van Grondelle, Biochim. Biophys. Acta 1657 (2004) 82.